ELSEVIER

Journal of Molecular Catalysis A: Chemical 192 (2003) 203–216

JOURNAL OF MOLECULAR CATALYSIS A: CHEMICAL

www.elsevier.com/locate/molcata

Modeling MoS_2 catalytic surface with simple clusters

Susana Lobos [a,b], Anibal Sierraalta [a,*], Fernando Ruette [a], Eloy N. Rodríguez-Arias [b]

[a] *Laboratorio de Química Computacional, Centro de Química, Instituto Venezolano de Investigaciones Científicas (IVIC), Apartado 21827, Caracas 1020-A, Venezuela*

[b] *Laboratorio de Modelaje en Catálisis, Departamento de Química, Universidad Simón Bolívar, Apartado 8900, Caracas 1080-A, Venezuela*

Received 11 March 2002; accepted 9 July 2002

Abstract

Theoretical calculations using a modified version of CNDO/UHF method to correct binding energies were carried out on a series of linear Mo_xS_y ($x = 3$; $y = 6$, 8, 10, 12, 14 and $x = 5$; $y = 12$, 14) and non-linear ($x = 3$, $y = 6$, 8, and $x = 5$, $y = 6$, 8, 10, 12, 14, 16, 18, 20) clusters. Results show the formation of S_2^- species on the surface and the existence of a Mo–Mo interaction. The HOMO orbitals are localized on mono-coordinate S atoms which shows that these atoms have electron-donating properties while the LUMO orbital is delocalized over all coordinatively unsaturated Mo atoms which presents electron-acceptor properties. It is shown that the non-linear clusters are better models for representation of MoS_2 catalysts, because they of their stability respect to the linear clusters.

Keywords: Parametric method; HDS; MoS_2; CNDO-UHF; Vacancies; Cluster

1. Introduction

It is well-known that the hydrodesulfurization (HDS) of hydrocarbons is an important catalytic process in the purification of petroleum products due to the high organosulfur compounds content in the heavy oil [1–8]. Different hydrogenation reactions occurs during the HDS processes such as

$$RSH + H_2 \rightarrow RH + H_2S \quad (1)$$

$$RSR + 2H_2 \rightarrow 2RH + H_2S \quad (2)$$

$$RSSR + 3H_2 \rightarrow 2RH + 2H_2S \quad (3)$$

Usually, industrial catalysts employed in hydrodesulfurization reactions are composed by molybdenum or tungsten sulfides supported on alumina and promoted with Ni or Co. These catalysts are complex because their highly anisotropic layered structure. Commonly, they are seen as slabs with a MoS_2-like structure and few layers. It is now agreed that the active sites are located at the edges of the lamellar structure, and the properties of the unsupported catalysts are roughly similar to those of supported systems. Thus, the problem of interaction between the active phase and the support can be avoided using an unsupported solids model [5,9]. Besides the hydrodesulfurization, the MoS_2 and its derivatives are also used in other catalytic reactions, such as isomerization [10], hydrogenation [11], methanation [12], Fischer–Tropsch [13], alcohol synthesis [14], hydrodenitrogenation (HDN) [15], coal liquefaction [16],

* Corresponding author. Tel.: +58-2-5041442; fax: +58-2-5041350.
E-mail address: asierral@ivic.ve (A. Sierraalta).

1381-1169/02/$ – see front matter
PII: S1381-1169(02)00418-1

in lubricant uses [17] and in nanotube technology [18]. Furthermore, this material is noteworthy due to its optical, magnetic, superconductive and electrical properties, etc. [19–21]. However, the chemical properties of Mo–S bonds in the microscopic structure are not well-known. Nevertheless, it is known what these properties depend on crystal plane, metal oxidation state, and surroundings [22–35]. All of these factors have strong influence on active sites that are associated with the anionic vacancies of the MoS_2 catalyst. These vacancies are formed on the MoS_2 catalyst during the pretreatment with H_2 or H_2/H_2S [36–38].

Quantum chemistry methods based on the neglect differential overlap (NDO) philosophy have been applied to catalytic reactions on transition metals [39–41]. However, these methods depends essentially on how well simulated the parametric functionals are. These parametric functionals are used to evaluate the components of the total energy expression [42–46] and the improvement of these methods is a difficult task because, the parametric functionals must obey the correct asymptotic behavior and the energy components must follow the basic theorems of quantum chemistry [46]. In addition, parameterization for transition metal systems is a very complicated process [43,47], because it has to deal with open shell systems in which several electronic states lay very close in energy. Nevertheless, it is possible to obtain reliable results without a deep parameterization using convenient theoretical tools. For example, a very reasonable evaluation of the interaction energies between atoms in a molecular system can be obtained by the calculation of parameterized diatomic binding energies [48].

In this work, we model the MoS_2 catalytic surface using Mo_xS_y discrete structures. The quantum chemistry behavior of the Mo–S bond in relation with its position into the molecular structure, the Mo oxidation state, the effect of S neighboring atoms, HOMO, and LUMO are analyzed.

2. Computational and theoretical details

A parametric method based on CNDO-UHF [49] was employed in this work. This includes several modifications [50,51] such as the calculation of diatomic binding energies and Mülliken population with orthogonal molecular orbitals, using the symmetric transformation of the orbitals. The standard atomic set of parameters employed herein is well described in a previous work [52].

It is well-known that CNDO overestimates binding energies [53,54]. Therefore, in order to amend the calculation of the total energy (E_T) and diatomic binding energies (DBE), a new parameterization per each bond was done. This new parameterization let to calculate reasonable total binding energies (TBE) based on a partition scheme of the TBE [52].

The E_T can be calculated in terms of parameterized DBEs (PDBEs) [55] as follows:

$$E_T = \sum_A \varepsilon_A^0 + \sum_{A>B} \mathrm{PDBE(A–B)} \quad (4)$$

$$\mathrm{PDBE(A–B)} = \alpha_{AB}\mathrm{DBE(A–B)} \quad (5)$$

and

$$\mathrm{TBE} = E_T - \sum_A \varepsilon_A^0 \quad (6)$$

where ε_A^0 corresponds to the energy of the free atom A. The parameters α_{AB} were obtained from the ratio between the accurate value (experimental or theoretical) of the bond dissociation energy (BDE) and the calculated DBE of the correspondent bond of the diatomic or polyatomic molecule, i.e. α_{AB} = BDE(A–B)/DBE(A–B). The values of the calculated parameters α_{AB} used herein are: $\alpha_{Mo–Mo} = 0.77$, $\alpha_{S–S} = 0.77$, and $\alpha_{Mo–S} = 0.52$. The α_{AB} values were obtained using BDE data taken from theoretical and experimental data [56–58]. As expected, this approach only gives semi-quantitative results, for example, the PDBE(C–H) for CH_4 and CH_3 molecules are 99.6 and 114.3 kcal/mol, respectively compared with the experimental values of 101.6 and 112.3 kcal/mol [59].

3. Surface model

It is well-known that the MoS_2 crystallite size depends on the preparation method. Normally, the crystallites size in ultra disperse particles is between 10 and 50 Å, for example, in those catalysts prepared by anchoring Mo complexes [3,60–62]. In catalysts prepared by impregnation, the particles size is around

100 Å [3]. Nevertheless, all of these particles, independent of the size, are catalytically actives. On the other hand, the HDS reaction occurs on edges of small slabs of MoS_2 [11,63], therefore, it is reasonable to use only few atoms to model a catalytic active surface.

Following assumptions were considered for the selection of a catalytic model surface: (a) the surface must have vacancies (completely exposed Mo sites), due to a pretreatment with H_2; (b) only single slab structures were chosen because the MoS_2 has a laminar structure with weak interlayer interaction (van der Waals interaction); (c) the electroneutrality principle of clusters must be obeyed, therefore, the total clusters charge is zero [3]; and (d) to study the change of Mo–S bond with the cluster size and surroundings, the central Mo atom (Mo_C) was chosen because it represent better a real active site than the other Mo atoms.

Almost all clusters used in this work are non-stoichiometric. The non-stoichiometry of the clusters constitutes a frequent problem in the theoretical modeling. Different solutions have been proposed in the literature, for example, to maintain the stoichiometry and the formal charges of the Mo (Mo^{4+}) and the S (S^{2-}) atoms some authors had used charged clusters

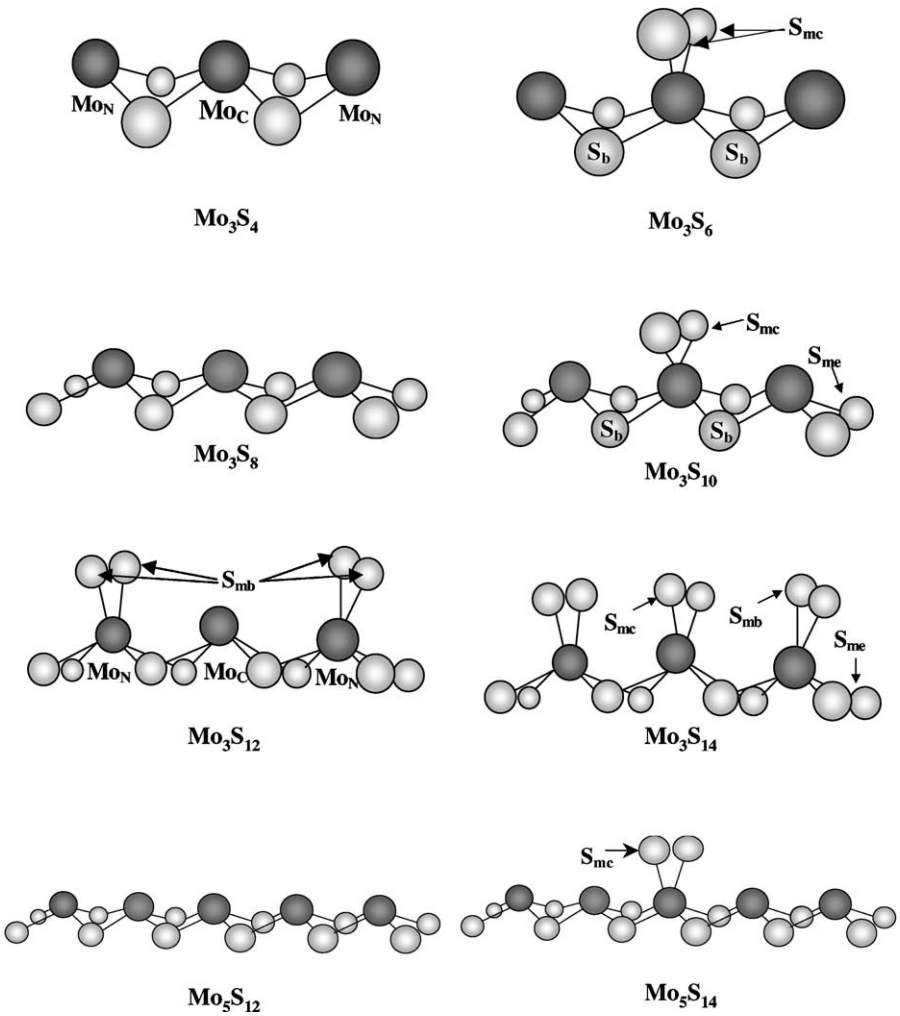

Fig. 1. Draw of the molecular structures used in this work for the linear Mo_xS_y systems ($x = 3$; $y = 4$, 6, 8, 10, 12, 14 and $x = 5$; $y = 12$, 14).

such as MoS_6^{8-} or $Mo_7S_{24}^{20-}$ [64], but these high negative charges are quite unrealistic [65]. Another adopted solution is to saturate the clusters with H atoms in such way to compensate the negative charge for example the $Mo_2S_{10}H_{12}$ cluster [66,67]. On the other hand, in a comparative study using DV-Xα between the Mo_3S_{14}, Mo_3S_6 and Mo_5S_{10} clusters, Rong and Qin [68] showed that the non-stoichiometry of the Mo/S ratio does not have a strong influence on the electronic properties. Ma and Schobert [41] using ZINDO showed too that the electronic properties of the Mo atoms does not change when going from stoichiometry clusters to non-stoichiometry ones.

From the assumptions mentioned above, two different types of molecular models were selected: linear and non-linear ones. The linear Mo_xS_y systems ($x = 3$; $y = 6$, 8, 10, 12, 14 and $x = 5$; $y = 12$, 14) are shown in Fig. 1. The difference between clusters is in the coordination of two mono-coordinated S atoms (S_{mc}) to the Mo_C atom. Having in mind that the MoS_2 surface is treated with H_2, we consider in our models several degrees of desulfurization, from a desulfurized surface (Mo_3S_4) to a total sulfurized surface (Mo_3S_{14}), as well as to intermediate cases. Different types of sulfur were included in the models: mono-coordinated on the border above the cluster (S_{mb}), on the edge below (S_{me}), and the bridge (S_b) bi-coordinated.

In the case of non-linear systems, Mo_xS_y ($x = 3$, $y = 6$, 8, and $x = 5$, $y = 6$, 8, 10, 12, 14, 16, 18, 20), a systematic construction of aggregates were also performed. Fig. 2 displays the non-linear systems studied herein. In these models, two rows of Mo atoms and two or three rows of S atoms were used. Three Mo and six S atoms compose the core of the non-linear system, forming a hexagon which have the correct stoichiometric formula (see Fig. 2).

4. Results and discussion

4.1. Linear clusters

Several non-stoichiometric molecular clusters with three and five Mo atoms and different sulfur contents were analyzed. The study was done starting from a totally desulfurized surface (Mo_3S_6, Mo-terminated $(3\,0\,\bar{3}\,0)$ edges), to a totally sulfurized one (Mo_3S_{14}, S-terminated $(1\,0\,\bar{1}\,0)$ edges). All of these linear structures (see Fig. 1) have an optimal spin multiplicity of five, except Mo_3S_8 and Mo_3S_{12} that are triplet and septuplet, respectively.

Several features can be obtained from Table 1: (a) distances R(Mo–S_{mc}) and R(S_{mc}–S_{mc}) present small variations with the cluster size; (b) the complete saturated edge sites with sulfur atoms (Mo_3S_{12}) have the longest Mo_C–S_{mc} and the smallest S_{mc}–S_{mc} distances; (c) PDBE(Mo_C–S_{mc}) values correlate with the R(Mo_C–S_{mc}) distance, i.e. the R(Mo_C–S_{mc}) decreases, as the PDBE(Mo_C–S_{mc}) increases; and (d) the distance R(S_{mc}–S_{mc}) and PDBE(S_{mc}–S_{mc}) are closer to the anion S_2^- than the neutral S_2 molecule. These facts suggest that the S_{mc} atoms behave like an activated S_2^- group. A similar structure of S–S bonds was reported for Mo–S and W–S compounds [60].

The bond orders (see Table 2) show that the interaction between the S_{mc} and S_b, with the Mo_C atom is through Mo-sp orbitals with an important participation of metal d orbitals. Free Mo atom has a $5s^14d^5$ configuration. However, in the linear aggregates, the Mo atom has a $5s^{0.3}5p^{0.3}4d^{4.7}$ configuration. It is clear therefore, that a charge transfer from Mo to S atoms occurs as well as an electronic reorganization, i.e. an spd re-hybridization. This facilitate the binding of several S atoms to one Mo atom. The central Mo (Mo_C) is bonded not only to S_{mc} and S_b, but to the neighbor

Table 1
Geometrical properties and PDBE values for Mo_C and S_{mc} atoms in linear clusters

Cluster	R(Mo_C–S_{mc}) (Å)	R(S_{mc}–S_{mc}) (Å)	PDBE(Mo_C–S_{mc}) (kcal/mol)	PDBE(S_{mc}–S_{mc}) (kcal/mol)
Mo_3S_6	2.30	2.17	−90.1	−59.5
Mo_3S_{10}	2.28	2.18	−91.3	−53.4
Mo_5S_{14}	2.27	2.19	−91.8	−57.4
Mo_3S_{14}	2.35	2.12	−81.8	−71.3
S_2^0	–	2.00	–	−101.5
S_2^-	–	2.08	–	−69.6

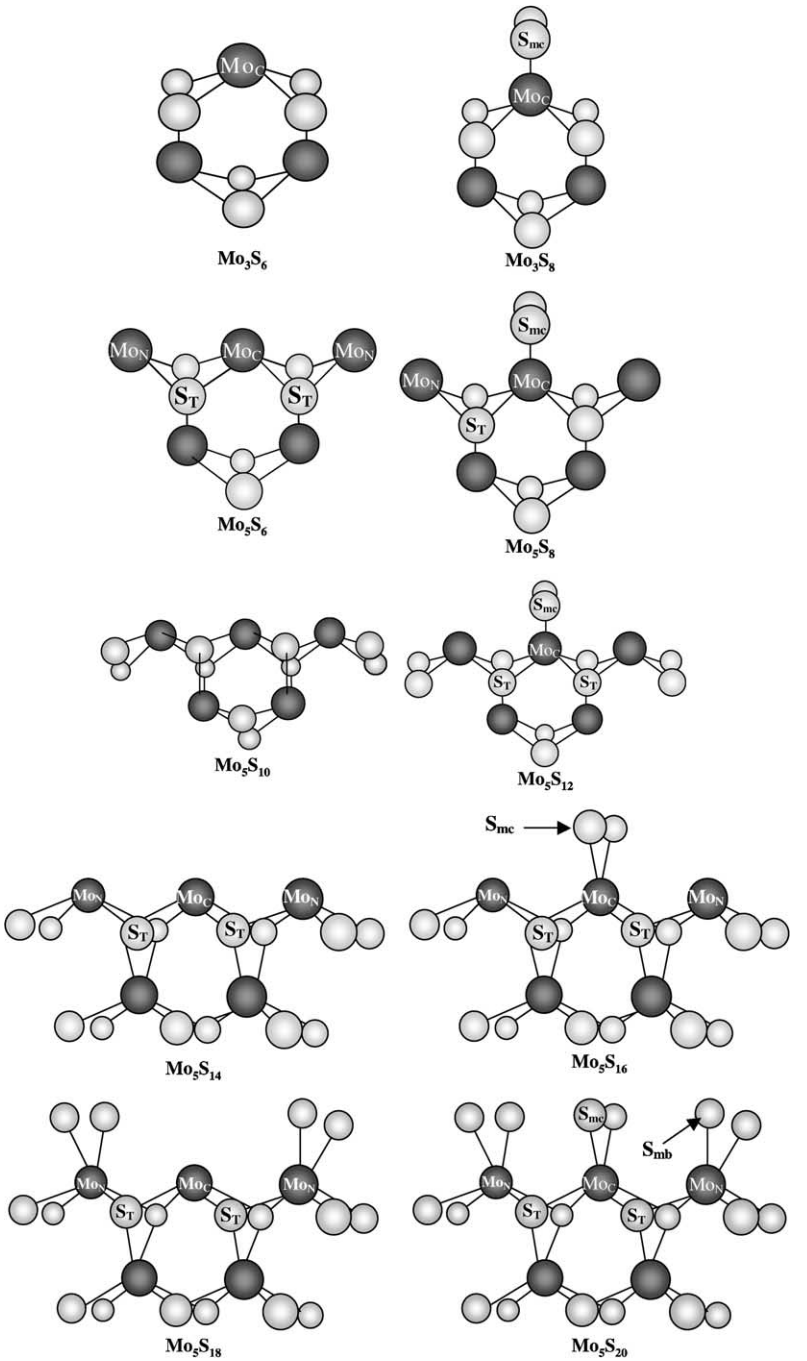

Fig. 2. Draw of the molecular structures used in this work for the non-linear systems, Mo_xS_y ($x = 3$, $y = 6$, 8, and $x = 5$, $y = 6$, 8, 10, 12, 14, 16, 18, 20).

Table 2
Partitioned bond orders (sp–sp and d–sp) for Mo–Mo and Mo–S bonds in linear clusters

Cluster	Mo_C–Mo_N		Mo_C–S_b		Mo_C–S_{mc}		S_{mc}–S_{mc}
	sp–sp	d–sp	sp–sp	d–sp	sp–sp	d–sp	sp–sp
Mo_3S_4	0.76	0.06	1.02	0.37	–	–	–
Mo_3S_6	0.70	0.05	0.95	0.39	0.93	0.45	0.87
Mo_3S_8	0.74	0.06	1.02	0.35	–	–	–
Mo_3S_{10}	0.69	0.04	0.94	0.39	0.94	0.45	0.85
Mo_5S_{12}	0.74	0.07	1.02	0.39	–	–	–
Mo_5S_{14}	0.69	0.06	0.93	0.38	0.94	0.40	0.76
Mo_3S_{12}	0.68	0.06	0.97	0.35	–	–	–
Mo_3S_{14}	0.65	0.05	0.94	0.35	0.88	0.38	1.04

Mo atoms (Mo_N) through sp–sp interactions. When the Mo_C–S_{mc} is formed a weakening of the Mo_C–S_b and Mo_C–Mo_N bonds occurs due to the redistribution of the electrons in the bonding structure.

The PDBE values in Table 3 clearly show, as well as the bond order values in the Table 2, that there is a Mo_C–Mo_N bond that is weaker than the Mo_C–S bond. The existence of Mo–Mo bond is not unusual, for example, the experimental Mo–Mo bond distance is 3.22 Å in the $[h^5\text{-}C_5H_5Mo(CO)_3]_2$ [69] complex. This distance is longer than the Mo–Mo distance (3.16 Å) in MoS_2 [70]. Therefore, one could expect an Mo–Mo bond in the MoS_2. Table 3 shows a general tendency, the Mo–S_b bonds (PDBE(Mo_C–S_b)) are stronger than the Mo_C–S_{mc} ones (see Table 1). This result in concordance with the experimental results [37,70], which show that S_{mc} atom is more labile than the S_b ones.

The calculated Mo_C–S_{mc} (2.27–2.35 Å) bond distances (Table 1) are shorter than those in the MoS_2 bulk (2.41 Å) [71]. This can be explained due to unsaturations in the small clusters sizes. The net charge on the Mo_C (see Table 3), as expected, increases when the coordination of the Mo_C atom increases. This shows that an oxidation process occurs on the Mo atom. The total net charge on two S_{mc} atoms is around $-0.6e$, indicating again that the S_{mc}–S_{mc} behaves like an activated S_2^- group, as shown previously.

Increasing the saturation of the neighbor Mo atoms affect the electronic distribution of the central Mo atom. The PDBE(Mo_C–Mo_N) is lower for Mo_3S_{12} than for Mo_3S_8, Mo_3S_4, and Mo_5S_{12} because the Mo_N atoms have to share their electrons with the S_{mb} atoms. A particular striking result is the interaction Mo_C–S_{mc} in the Mo_3S_{14} molecular cluster. The S_{mc} atoms are less bonded to the central Mo in the Mo_3S_{14} than in the other linear clusters. As a consequence, the PDBE(S_{mc}–S_{mc}) is higher and the PDBE(Mo_C–S_{mc}) is lower than in the other clusters, see Table 1. For Mo_3S_{14} cluster, the central Mo atom has one unpaired electron, therefore, two S_{mc} atoms are bonded to the Mo_C through one electron instead of two, as a result the interaction between the Mo_C and the S_{mc} atoms is weaker.

The interaction between the central Mo and the S atoms can be analyzed as a reaction between one S_2 molecule with a clean MoS_2 surface, according to the following reactions scheme:

$$Mo_3S_8 + S_2 \rightarrow Mo_3S_{10},$$
$$\Delta E = -141.1\ \text{kcal/mol} \quad (7)$$

Table 3
PDBEs and net charges on the Mo_C and the S_{mc} atoms for linear clusters

Cluster	PDBE(Mo_C–Mo_N) (kcal/mol)	PDBE(Mo_C–S_b) (kcal/mol)	PDBE[Mo–S][a] (kcal/mol)	Charge on Mo_C	Charge on S_{mc}
Mo_3S_4	−76.0	−115.3	−114.7	+0.75	–
Mo_3S_6	−54.5	−93.3	−93.7	+1.50	−0.30
Mo_3S_8	−55.8	−94.2	−93.1	+0.68	–
Mo_3S_{10}	−59.8	−92.1	−92.7	+1.50	−0.28
Mo_5S_{12}	−52.1	−95.6	−98.5	+0.78	–
Mo_5S_{14}	−48.2	−89.7	−92.9	+1.39	−0.24
Mo_3S_{12}	−46.4	−94.5	−96.7	+0.74	–
Mo_3S_{14}	−41.9	−92.3	−90.7	+1.46	−0.28

[a] Mean value of the PDBE(Mo–S) in the cluster.

$$Mo_3S_{12} + S_2 \rightarrow Mo_3S_{14},$$
$$\Delta E = -124.5\,\text{kcal/mol} \quad (8)$$

Again, the saturation with S atoms of the neighbor Mo atoms drastically affect the properties of the linear model, lowering the adsorption energy (reaction (8)). This shows the importance of the neighbor atoms. The quantum properties of Mo_3S_8, model corresponds to a clean Mo surface in the $(3\,0\,\bar{3}\,0)$ plane of the MoS_2, while the properties and the DE of Mo_3S_{12} to Mo_3S_{14} correspond to the $(1\,0\,\bar{1}\,0)$ plane. From the analysis of reaction energies, it is clear that the adsorption of a S_2 molecule is stronger in the $(3\,0\,\bar{3}\,0)$ plane than in a Mo vacancy localized in the $(1\,0\,\bar{1}\,0)$ plane (reactions (7) and (8)).

Considering the following reactions:

$$Mo_3S_8 + 2S_2 \rightarrow Mo_3S_{12},$$
$$\Delta E = -280.1\,\text{kcal/mol} \quad (9)$$

$$Mo_3S_{10} + 2S_2 \rightarrow Mo_3S_{14},$$
$$\Delta E = -263.5\,\text{kcal/mol} \quad (10)$$

From reactions (9) and (10), values of −140.1 and −131.8 kcal/mol for the adsorption energy of one S_2 molecule were obtained. Comparing these values with the adsorption energy of reaction (8), one can observe the effect of the neighbor S atoms in the adsorption process (compare reactions (9) and (10)). On the other hand, plotting the calculated total binding energy (TBE) of the linear structures versus total number of Mo–S bonds, a linear relationship is obtained, as shown in Fig. 3. The value of the slope is −107.6 kcal/mol per bond. This value is higher than most of the average values given in Table 3 because of the formation of S–S bonds and the weakening of Mo–Mo interactions have to be considered.

4.2. Non-linear clusters

As in the previous case, a systematic analysis of several non-linear and non-stoichiometric clusters were done. The Mo–S_{mc} and S_{mc}–S_{mc} distances were only optimized for these clusters (see Fig. 2). In the two rows structures, an optimal multiplicity of three was found, except for the Mo_5S_{18}, which is a quintuplet. Table 4 shows that the interatomic S_{mc}–S_{mc} and Mo_C–S_{mc} distances are almost independent of the size of the cluster. In general, the values PDBE for the Mo–S_{mc} and S_{mc}–S_{mc} bonds are stronger than those found for the linear aggregate models. There is also an important Mo–Mo interaction (see Table 5) that is weaker than in the linear ones.

Two S atoms bonded to the central Mo atom (Mo_C atom) produces a charge transfer from the Mo atom to the S_{mc} atoms, as expected. In this sense, the non-linear clusters the electronic charge density on S atoms is in general, greater than in linear ones, see Table 5. Table 6 shows that the Mo–Mo interaction occurs mainly through the 5s5p orbitals since the 4d orbitals are compromised in the Mo–S bonding. These orbitals represent a 30% of the Mo–S bond through d–sp interactions. A clear decrease of sp–sp and d–sp bond is observed in the non-linear clusters with respect to linear ones. Comparing non-linear with linear structures, the S_{mc}–S_{mc} bonds are weaker and the negative charge on S_{mc} atoms is higher in the former. For example, the S_{mc}–S_{mc} bond order in Mo_3S_{14} (liner) is 1.04 and 0.88 for Mo_5S_{20} (non-linear) with S_2 charges of −0.56 and −0.76 a.u., respectively.

Considering the following set of reactions:

$$Mo_3S_6 + S_2 \rightarrow Mo_3S_8,$$
$$\Delta E = -113.9\,\text{kcal/mol} \quad (11)$$

Table 4
Geometrical properties and PDBE values for Mo_C and S_{mc} atoms in non-linear clusters

Cluster	$R(Mo_C–S_{mc})$ (Å)	$R(S_{mc}–S_{mc})$ (Å)	PDBE($Mo_C–S_{mc}$) (kcal/mol)	PDBE($S_{mc}–S_{mc}$) (kcal/mol)
Mo_3S_8	2.31	2.16	−90.8	−61.5
Mo_5S_8	2.31	2.15	−99.5	−70.7
Mo_5S_{12}	2.30	2.16	−96.2	−62.7
Mo_5S_{16}	2.29	2.16	−96.4	−60.7
Mo_5S_{20}	2.32	2.16	−90.0	−86.7

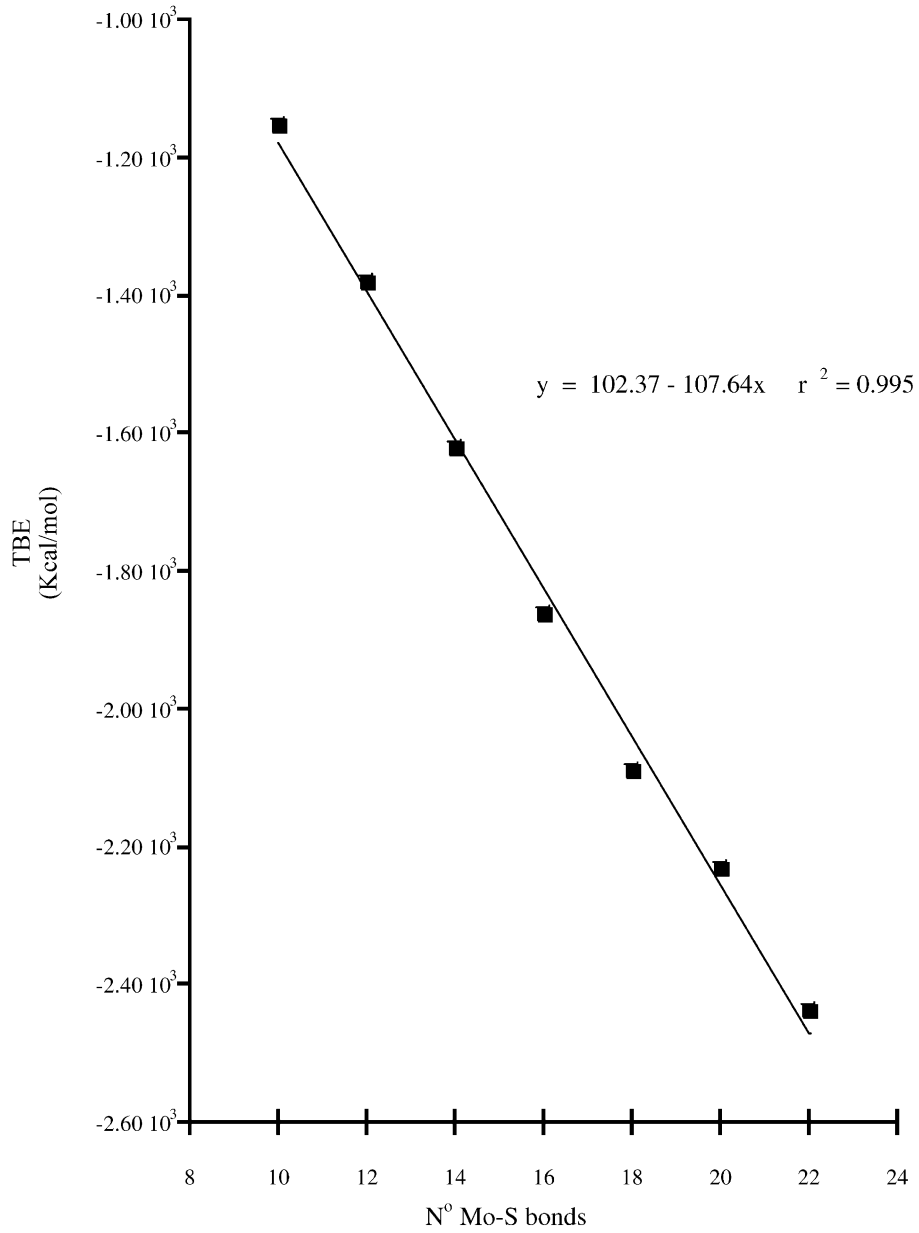

Fig. 3. Plot of the calculated total binding energy (TBE) of the linear structures vs. total number of Mo–S bonds.

$$Mo_5S_6 + S_2 \rightarrow Mo_5S_8, \quad \Delta E = -153.6\,\text{kcal/mol} \tag{12}$$

$$Mo_5S_{10} + S_2 \rightarrow Mo_5S_{12}, \quad \Delta E = -174.1\,\text{kcal/mol} \tag{13}$$

$$Mo_5S_{14} + S_2 \rightarrow Mo_5S_{16}, \quad \Delta E = -130.8\,\text{kcal/mol} \tag{14}$$

$$Mo_5S_{18} + S_2 \rightarrow Mo_5S_{20}, \quad \Delta E = -108.8\,\text{kcal/mol} \tag{15}$$

Table 5
PDBEs and net charges on the Mo_C, S_T and S_{mc} atoms for non-linear clusters

Cluster	PDBE(Mo_C–Mo_N) (kcal/mol)	PDBE(Mo_C–S_T) (kcal/mol)	PDBE[Mo–S][a] (kcal/mol)	Charge on Mo_C	Charge on S_{mc}
Mo_3S_6	–	–	−90.8	+0.89	–
Mo_3S_8	–	–	−88.7	+1.39	−0.25
Mo_5S_6	−55.6	−88.7	−93.1	+0.64	–
Mo_5S_8	−51.5	−84.1	−92.7	+1.46	−0.38
Mo_5S_{10}	−48.5	−87.1	−92.0	+0.65	–
Mo_5S_{12}	−44.7	−82.6	−88.2	+1.40	−0.34
Mo_5S_{14}	−50.8	−88.9	−93.6	+0.59	–
Mo_5S_{16}	−42.1	−83.4	−89.9	+1.47	−0.33
Mo_5S_{18}	−46.5	−84.3	−90.1	+0.69	–
Mo_5S_{20}	−34.3	−84.7	−91.1	+1.40	−0.38

[a] Mean value of the PDBE(Mo–S) in the cluster.

It is clear from reactions (11)–(13) that the reaction energy (DE) increases as the size of the aggregate increases. On the other hand, for the set of reactions (13)–(15), the energy reaction decreases as the S content increase in the clusters. It shows that increasing the saturation with S atoms affect the chemical properties, such as the reaction energy $Mo_xS_y + S_2$.

In similar way, a plot of the calculated total binding energy (TBE) for the non-linear structures versus the total number of Mo–S bonds shows a linear relation (see Fig. 4). The value of the slope −118.6 kcal/mol per bond corresponds to the formation energy of one Mo–S bond. This value is higher than the corresponding of the clusters of the linear structures, because there is an extra stabilization energy due to the cyclic structure. In the non-linear structures, there are more bonds per atom than in a linear one. For example, Mo_3S_6 and Mo_3S_8 clusters present 10 and 12 Mo–S bonds compared with 12 and 14 bonds of the corresponding non-linear clusters. In addition, there are three-coordinated S atoms and two more Mo interactions in clusters of five Mo atoms that help to stabilize these structures. The S–S interactions is important only for edges sulfurs, therefore, if one substract the S–S contributions (half of S–S bond per Mo–S bond) it is possible to make a comparison with the bulk. The average value of S–S bond was −34.1 kcal/mol in Mo_5S_{20} and result in −84.5 kcal/mol per Mo–S

Table 6
Partitioned bond orders (sp–sp and d–sp) for non-linear clusters

Cluster	Mo_C–Mo_N		Mo_C–S_T		Mo_C–S_{mc}		S_{mc}–S_{mc}
	sp–sp	d–sp	sp–sp	d–sp	sp–sp	d–sp	sp–sp
Mo_3S_6	–	–	1.00	0.32	–	–	–
Mo_3S_8	–	–	0.92	0.38	0.97	0.41	0.83
Mo_5S_6	0.67	0.06	0.92	0.34	–	–	–
Mo_5S_8	0.63	0.04	0.84	0.33	0.94	0.41	0.92
Mo_5S_{10}	0.67	0.04	0.93	0.32	–	–	–
Mo_5S_{12}	0.63	0.04	0.83	0.38	0.96	0.43	0.77
Mo_5S_{14}	0.71	0.05	0.93	0.33	–	–	–
Mo_5S_{16}	0.62	0.04	0.84	0.35	0.96	0.41	0.79
Mo_5S_{18}	0.63	0.06	0.88	0.37	–	–	–
Mo_5S_{20}	0.59	0.05	0.82	0.35	0.89	0.35	0.88

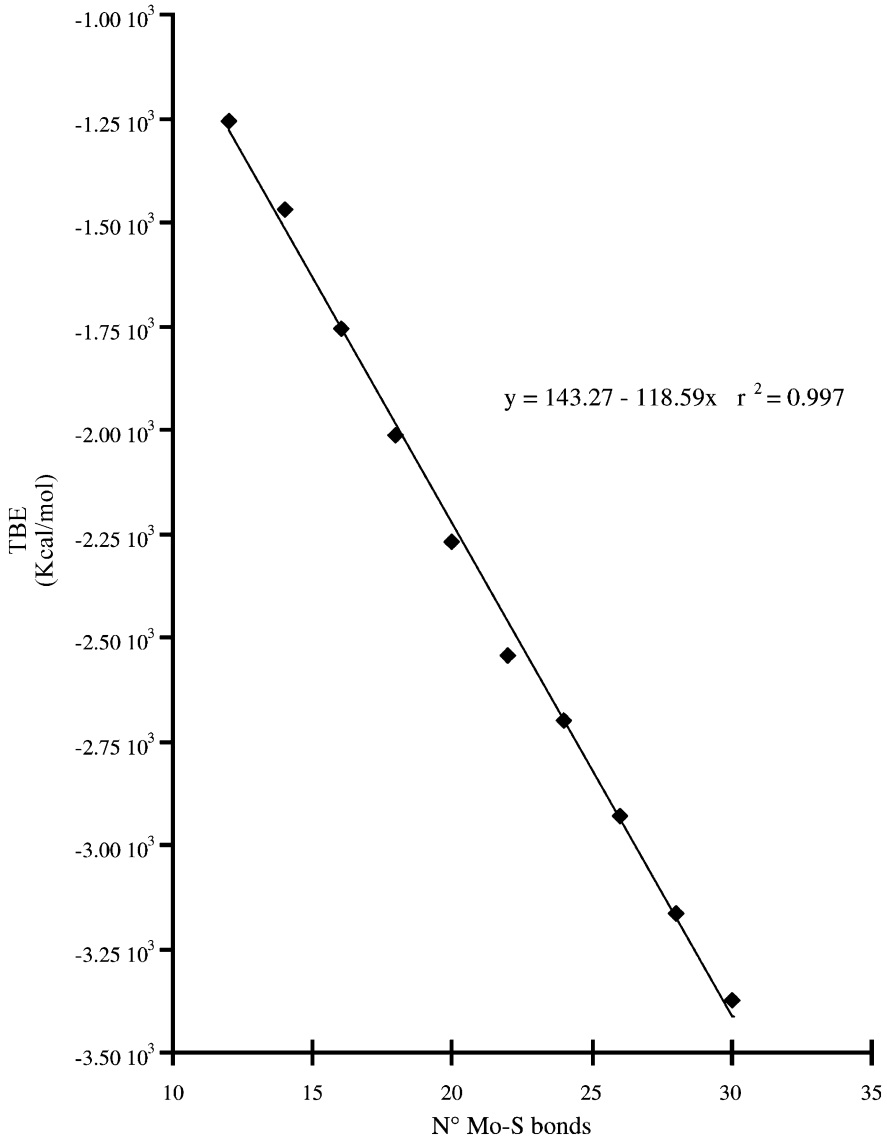

Fig. 4. Plot of the calculated total binding energy (TBE) for the two-layer structures vs. the total number of Mo–S bonds.

bond. This value is close to the reported value of −87.9 kcal/mol for the energy of sulfur-extraction calculated by using DFT approach [58].

In order to estimate the energy for the vacancy formation, the reaction

$$Mo_nS_m + H_2 \rightarrow Mo_nS_{m-1} + H_2S \quad (16)$$

is divided in a two-step reaction. The first correspond to the extraction of one S atom and the second to the H_2S formation from molecular H_2 and atomic S:

$$Mo_nS_m \rightarrow Mo_nS_{m-1} + S \quad (17)$$

$$S + H_2 \rightarrow H_2S \quad (18)$$

Using the value of the slope of Fig. 4 and the calculated total binding energy for the reaction (18) (−159.8 kcal/mol), we obtain a value of −40.9 kcal/mol for reaction (16). This value is

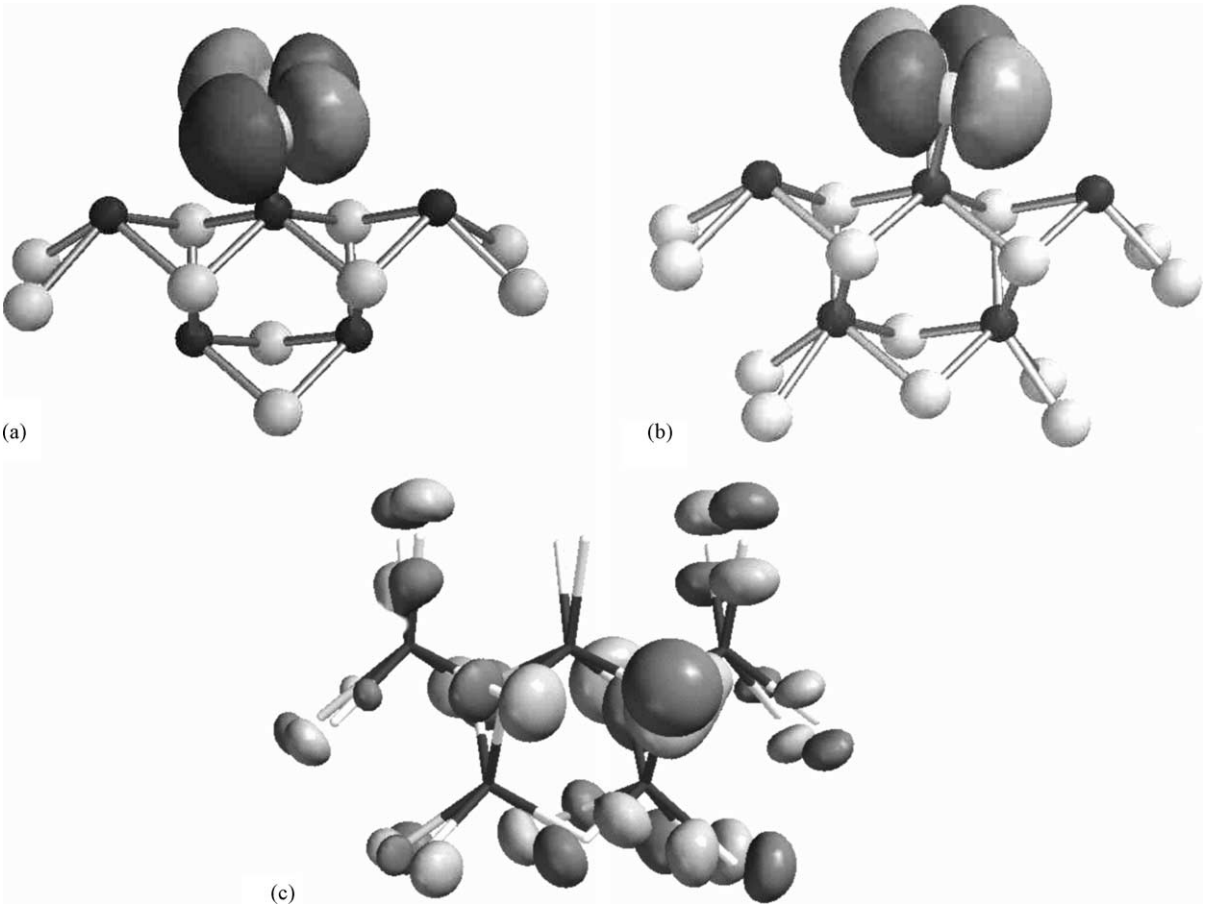

Fig. 5. Schematic representation of two-layer aggregates HOMO orbital.

higher than the reported using DFT calculations of −30.1 kcal/mol [24].

In general, for non-linear aggregates, the HOMO is highly localized over the S atoms, as shown in Fig. 5. Fig. 5a and b shows that this orbital is the anti-bonding combination of two atomic p-type orbitals that belongs to the S_{mc} atoms. In the case of totally saturated clusters, the HOMO is delocalized over the whole structure (see Fig. 5c). Since the HOMO is localized in unsaturated aggregates and no localized in saturated aggregates (Fig. 5a and b), the reactivity of both aggregates could be different, but concentrated over the S atoms and not over the metallic centers. Taken into account the localization of the HOMOs and the electronic charge of these S atoms, it is possible to explain, partially, the mechanism of the H_2 dissociation. Since the S_{mc} atoms are negatively charged and the HOMO is localized over these atoms, it is very feasible that a charge transfer occurs from the S_{mc} atoms to the H_2 anti-bonding σ^* orbital, which makes more easy the H_2 dissociation and formation of S–H bond. These results are in agreement with previously published ones [23] that show that the addition of molecular H_2 to two adjacent sulfur atoms is a favorable process. Due to the different shapes of the HOMO in saturated and unsaturated aggregates the mechanism of vacancies formation can be different for both aggregates. For saturated aggregates, the H_2 molecule could first attacks any of S atoms, the S_{mc}, S_{mb}, S_{me}, S_b and the tricoordinate ones. After the vacancy formation the HOMO change its shape (unsaturated aggregate, Fig. 5a and b), therefore, the H_2 will interact preferentially with the S_{mc}.

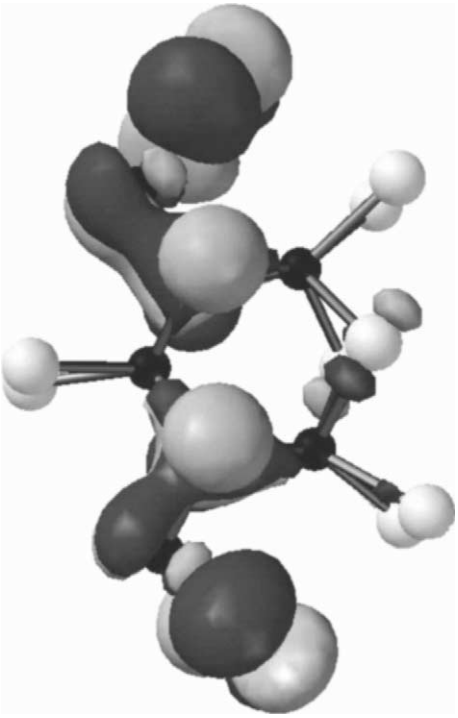

Fig. 6. Schematic representation of LUMO orbital.

On the other hand, the LUMO orbital is mainly located on the coordinatively unsaturated Mo atoms (Mo_N atoms, see Fig. 6). This indicates that these Mo atoms have electron-accepting properties while the S_{mc} atoms, due to the localization of the HOMO, have electron-donating properties. Ma and Schobert [41] using ZINDO program reported that the LUMO orbital of a $M_{10}S_{18}$ cluster is delocalized over the whole structure, but similar to our results, concentrated on unsaturated Mo atom. They concluded, therefore that the electron-acceptor properties of this atom let the flat adsorption of the thiophene molecule. Both factors (the localization of the HOMO and the LUMO orbitals) help to understand the HDS mechanism. Due to the LUMO is localized over the unsaturated Mo atoms, the thiophene molecule can coordinate to these Mo atoms while the neighbor S atoms can donate charge to the thiophene ring facilitating the breaking of the ring, as shown schematically in Fig. 7.

Delmon and coworkers [33], using ab initio calculations with a small basis set in a $Mo_{27}S_{54}$ cluster, found that the Mo atoms on the corner have both

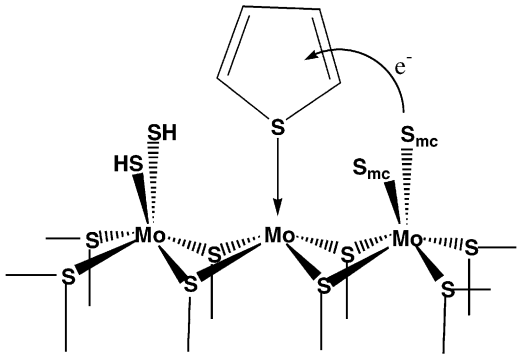

Fig. 7. Schematic representation of electron transfer from S atoms to the adsorbed thiophene molecule.

electron-accepting and donating properties, which is in agreement with our results. Nevertheless, they reported that the unsaturated central Mo atom (Mo_C) has very little participation in the LUMO orbital; therefore, this atom does not have electron-accepting properties. Our results, as well as those of [41], show that the LUMO is mainly localized over all coordinatively unsaturated Mo atoms. This disagreement could be explained by the fact that the semi-empirical approaches include in some degree the electronic correlation [43,46], and ab initio calculations with minimum basis sets are less accurate than semi-empirical ones [72].

5. Conclusions

(a) Once more, the use of energy partition and the parameterization of CNDO method using diatomic binding energies arise as a good tool for studying energetic interactions in catalytic systems.
(b) The linear clusters are less stable than the non-linear ones, because more bonds per number of atoms are observed in the later. It is convenient to use non-linear clusters with two rows of Mo atom to simulate MoS_2 surface catalyst.
(c) Changes in PDBEs, bond orders and charges on the Mo and S atoms are, in general, small for different types of aggregates, except for the very unsaturated ones.
(d) Formation of S–S bonds and S–Mo–S bonds on the surface are important for the formation of vacancies on the surface. It is proposed that a species

of S_2^- is formed on the $(1\,0\,\bar{1}\,0)$ surface plane. An important Mo–Mo interaction was also found.

(e) The shape and localization of the HOMO orbital depend on the size and sulfur saturation of clusters. HOMO is localized over the S_{mc} atoms, which shows that these S atoms are the electron-donating sites of the MoS_2 catalyst.

(f) The LUMO orbital is delocalized over all unsaturated Mo atoms, therefore, these atoms are principally electron-accepting sites.

Acknowledgements

The authors gratefully acknowledged (MTC) G-9700667, S1-2637 (E.N.R-A), CONICIT S1-96001399 grant (A.S.) for the financial support. They also thank Dr. Alejandro Arce for helpful discussions.

References

[1] R. Prins, V.H.J. de Beer, G.A. Somorjai, Catal. Rev.-Sci. Eng. 31 (1989) 1.
[2] P. Ratnasamy, S. Sivasanker, Catal. Rev.-Sci. Eng. 22 (1980) 401.
[3] A. Startsev, Catal. Rev.-Sci. Eng. 37 (1995) 353.
[4] F.E. Massoth, Adv. Catal. 27 (1978) 265.
[5] X.S. Li, Q. Xin, X.X. Guo, P. Grange, B. Delmon, J. Catal. 137 (1992) 385.
[6] R.J. Angelici, Polyhedron 16 (1997) 3073.
[7] S.C. Schuman, H. Shalit, Catal. Rev. 4 (1970) 425.
[8] R.R. Chianelli, M. Daaage, M.J. Ledoux, Adv. Catal. 40 (1994) 177.
[9] A.P. Raje, S.-J. Liaw, R. Srinivasan, B.H. Davis, Appl. Catal. A 150 (1997) 297.
[10] W.K. Hall, in: H.F. Barry, T.C.H. Mitchell (Eds.), Proceedings of the 4th International Conference on the Chemistry, uses if Molybdenum, Climax Molybdenum Co., Ann Arbor, MI, 1982, p. 224.
[11] K.I. Tanaka, T. Okuhari, J. Catal. 78 (1982) 155.
[12] B.K. Miremadi, S.R. Morrison, J. Catal. 103 (1987) 334.
[13] W.P. Dianis, Appl. Catal. 30 (1987) 99.
[14] T.Y. Park, Y.G. Kim, Ind. Eng. Chem. Res. 36 (1997) 5246.
[15] M.M. Luchsinger, B. Bozkurt, A. Akgerman, C.P. Janzen, W.P. Addiego, M.Y. Darensbourg, Appl. Catal. 68 (1991) 229.
[16] L. Artok, O. Erbatur, H.H. Schobert, Fuel Proc. Technol. 47 (1996) 153.
[17] T.D. Durbin, J.R. Lince, S.V. Didziulis, D.K. Stuck, J.A. Yarmoff, J. Vac. Sci. Technol. A 10 (1991) 2529.
[18] M. Remskar, A. Mrzel, Z. Skraba, A. Jesih, M. Ceh, J. Demsar, P. Stadelmann, F. Lévy, D. Mihailovic, Science 292 (2001) 479.
[19] D. Yang, S. Jiménez-Sandoval, W.M.R. Divigalpitiya, J.C. Irwin, R.F. Frindt, Phys. Rev. B 43 (1991) 12053.
[20] H. Wise, Polyhedron 5 (1986) 145.
[21] W.M.R. Divigalpitiya, R.F. Frindt, S.R. Morrison, Science 246 (1989) 369.
[22] S.Y. Li, J.A. Rodríguez, J. Hrbek, H.H. Huang, G.-Q. Xu, Surf. Sci. 366 (1966) 29.
[23] A. Sierraalta, F. Ruette, J. Mol. Catal. A 109 (1996) 227.
[24] L.S. Byskov, B. Hammer, J.K. Nørskov, B.S. Clausen, H. Topsøe, Catal. Lett. 47 (1997) 177.
[25] K.E. Dungey, M.D. Curtis, J.E. Penner-Hahn, Chem. Mater. 10 (1998) 2152.
[26] P. Raybaud, J. Hafner, G. Kresse, H. Toulhoat, Phys. Rev. Lett. 80 (1998) 1481.
[27] P. Raybaud, J. Hafner, G. Kresse, H. Toulhoat, Surf. Sci. 407 (1998) 237.
[28] H. Toulhoat, P. Raybaud, S. Kasztelan, G. Kresse, J. Hafner, Catal. Today 50 (1999) 629.
[29] J. Heising, M.G. Kanatzidis, J. Am. Chem. Soc. 121 (1999) 638.
[30] L.S. Byskov, J.K. Nørskov, B.S. Clausen, H. Topsøe, Catal. Lett. 64 (2000) 95.
[31] V. Alexiev, R. Prins, T. Weber, Phys. Chem. Chem. Phys. 2 (2000) 1815.
[32] S. Cristol, J.F. Paul, E. Payen, D. Bougeard, S. Clémendot, F. Hutschka, J. Phys. Chem. B 104 (2000) 11200.
[33] Y.-W. Li, X.-Y. Pang, B. Delmon, J. Phys. Chem. 104 (2000) 11375.
[34] M. Breysse, G. Berhault, S. Kasztelan, M. Lacroix, F. Maugé, G. Perot, Catal. Today 66 (2001) 15.
[35] A. Sierraalta, A. Herize, R. Añez, J. Phys. Chem. A 105 (2001) 6519.
[36] S. Kasztelan, H. Toulhoat, J. Grimblot, J.P. Bonnelle, Appl. Catal. 13 (1984) 127.
[37] A. Wambeke, L. Jalowiecki, S. Kasztelan, J. Grimblot, J.P. Bonnelle, J. Catal. 109 (1988) 320.
[38] E. Diemann, Th. Weber, A. Müller, J. Catal. 148 (1994) 288.
[39] M.C. Zerner, in: K.B. Lipkowistz, D.B. Boyd (Eds.), Reviews in Computational Chemistry, vol. 2, VCH, New York, 1990.
[40] F. Ruette, A. Sierraalta, A. Hernández, in: F. Ruette (Ed.), Quantum Chemistry Approaches to Chemisorption, Heterogeneous Catalysis, Kluwer Academic Publishers, Dordrecht, 1992, p. 320, references therein.
[41] X. Ma, H.H. Schobert, J. Mol. Catal. A 160 (2000) 409.
[42] M. Romero, J. Primera, M. Sánchez, A. Sierraalta, S. Brassesco, J. Bravo, F. Ruette, Folia Chim. Theor. Latina 23 (1995) 45.
[43] M. Romero, M. Sánchez, A. Sierraalta, L. Rincón, F. Ruette, J. Chem. Inform. Comput. Sci. 39 (1999) 543.
[44] J. Primera, M. Sánchez, M. Romero, A. Sierraalta, F. Ruette, J. Mol. Struct. (Theochem.) 469 (1999) 177.
[45] F. Ruette, F.M. Poveda, A. Sierraalta, M. Sánchez, E.N. Rodríguez-Arias, J. Mol. Catal. A: Chem. 119 (1997) 335.
[46] F. Ruette, C. González, A. Octavio, J. Mol. Struct. (Theochem.) 537 (2001) 17.
[47] L. Rodríguez, F. Ruette, J. Mol. Struct. (Theochem.) 287 (1993) 179.
[48] F. Ruette, F.M. Poveda, A. Sierraalta, J. Rivero, Surf. Sci. 249 (1996) 241.

[49] J.A. Pople, D.L. Beveridge, Approximate Molecular Orbital Theory, McGraw-Hill, New York, 1970.
[50] A.J. Hernández, F. Ruette, E.V. Ludeña, J. Mol. Catal. 39 (1987) 21.
[51] F. Ruette, G.L. Estiú, A.J. Jubert, R. Pis-Diez, Rev. Ven. Soc. Catal. 57 (1999) 13.
[52] F. Ruette, N. Valencia, R. Sánchez-Delgado, J. Am. Chem. Soc. 111 (1989) 40.
[53] A.E. Gaínza, E.N. Rodríguez, F. Ruette, J. Mol. Catal. 85 (1993) 345.
[54] E.N. Rodríguez-Arias, A.E. Gainza, A.J. Hernández, P.S. Lobos, F. Ruette, J. Mol. Catal. A: Chem. 102 (1995) 163.
[55] B. Griffe, A. Sierraalta, F. Ruette, J.L. Brito, J. Mol. Catal. 168 (2001) 265.
[56] P.M. Atha, L.H. Hillier, M.F. Guest, Chem. Phys. Lett. 75 (1980) 84.
[57] R.C. Weast (Ed.), Handbook of Chemistry, Physics, 53rd Edition, CRC Press, Cleveland, OH, 1973, p. F-183.
[58] H. Topsoe, B.S. Clausen, N.Y. Topsoe, J.K. Norskov, C.V. Ovesen, C.J.H. Jacobsen, Bull. Soc. Chim. Belg. 104 (1995) 283.
[59] J.E. Huheey, Inorganic Chemistry Principles of Structure and Reactivity, Harper & Row, New York, 1975, p. 692.
[60] A. Müller, Polyhedron 5 (1986) 323.
[61] E. Diemann, A. Branding, A. Müller, Bull. Soc. Chim. Belg. 100 (1991) 961.
[62] V.P. Fedin, J. Czyzniewska, R. Prins, T. Weber, Appl. Catal. A 213 (2001) 259.
[63] S. Helveg, J.V. Lauritsen, E. Lægsgaard, I. Stengaard, J.K. Nørskov, B.S. Clausen, H. Topsøe, F. Besenbacher, Phys. Rev. Lett. 84 (2000) 951.
[64] A.B. Anderson, Z.Y. Al-Saigh, W.K. Hall, J. Phys. Chem. 92 (1988) 809.
[65] Y.-W. Li, X.-Y. Pang, B. Delmon, J. Mol. Catal. A: Chem. 169 (2001) 259.
[66] I.I. Zakharov, A.N. Startsev, G.M. Zhidomirov, J. Mol. Catal. A: Chem. 119 (1997) 437.
[67] I.I. Zakharov, A.N. Startsev, J. Phys. Chem. B 104 (2000) 9025.
[68] C. Rong, X. Qin, J. Mol. Catal. 64 (1991) 321.
[69] F.A. Cotton, G. Wilkinson, Advanced Inorganic Chemistry, 3rd Edition, Interscience, New York, 1972, p. 548.
[70] L. Jalowiecki, A. Aboulaz, S. Kasztelan, J. Grimblot, J.P. Bonnelle, J. Catal. 102 (1989) 108.
[71] A. Wold, K. Dwight, Solid State Chemistry, Chapman & Hall, New York, 1993, p. 186.
[72] M. Karplus, J. Phys. Chem. 94 (1990) 5435.